A Numerical Simulation on the Transient Flow of Gas-steam Mixture in a Canister

Advisor: Prof. Jeong Soo Kim

by
Bhushan Ashok Bhosale

A dissertation submitted in partial fulfillment of the requirements
for the degree of

Master of Engineering

in Department of Mechanical Engineering, The Graduate School,
Pukyong National University

February 2017

Bhushan Ashok Bhosale 의 공학석사 학위논문을 인준함.

2017년 2월 24일

주 심 공학박사 권오붕 (인)

위 원 공학박사 배대석 (인)

위 원 공학박사 김정수 (인)

Contents

Nomenclature

ρ	Density of gases
ρ_m	Density of mixture
u_i	Velocity of gases
$\vec{u}_m$	Mass-averaged velocity of the mixture
ρg	Gravitational body force
F	External body force
P	Pressure
E	Total energy
μ_t	Turbulent viscosity
μ_m	Viscosity of mixture
I	Unit tensor
T	Temperature
K	Thermal conductivity
K_t	Turbulent thermal conductivity
h_k	Sensible enthalpy
k	Turbulent kinetic energy
ε	Turbulent dissipation rate
ω	Specific dissipation rate
C_p	Specific heat
M	Mach number
R	Universal gas constant

A Numerical Simulation on the Transient Flow of Gas－steam Mixture in a Canister

Bhushan Ashok Bhosale

Department of Mechanical Engineering, Graduate School

Pukyong National University

Abstract

The main objective of this research work is to analyze the complicated two-dimensional and three-dimensional flow structure created by the hot jet impingement on the canister walls and predict the pressure, velocity and temperature distribution inside a canister. These flow features inside the canister are mainly caused by the compressible flow. In this research work, a single and two-phase model is proposed in which the working fluid is taken as hot air (1,200 K) at an ideal gas state and a mixture of air and water vapor respectively. In order to examine the flow physics inside a canister for a single and two-phase model, the computer numerical simulation with two-equation standard k-ε and two equation SST turbulence model with the combination of

discrete phase model is used respectively. The accumulation of the hot air and a mixture of hot air with water vapor inside a canister develops into the pressurization which may cause the missile to lift and force it out from the canister. The entrance of the working fluid for both the cases inclines to the canister at an angle of 45° to prevent the direct jet-impinging in the sidewalls. The computational results with the turbulence models mentioned fairly well predict the pressure, velocity and temperature distribution in the canister.

1. Introduction

A routine of techniques has been built up to analyze the launching technology of the missile. For operational convenience, missiles are launched from the canister. The canister is a cylindrical container for holding, carrying, storing and launching of missiles. During storage and launching, the canister is subjected to internal and external pressures. Flight conditions govern the design of most of a ballistic missile structures. In the case of canister launches missiles, loads incurred during the launch phase can exceed to those limits which are obtained in flight. It is necessary to accurately predict these loads, therefore every launch phase must be thoroughly analyzed. Canister-launched techniques are generally classified in two categories, self-eject launch and gas eject launch. Within these two techniques, each with its own particular benefits and problems. Several ejection techniques were introduced before by many researchers such as gas-steam ejection, gas ejection with respect to the ejection power system, structure, change of pressure and acceleration, velocity and temperature.

One of the most promising gas eject technique is the use of a hot gas generator to provide the force to drive the missile out of the canister. In this operation, a solid propellant gas generator is fired up in the closed volume below the missile in the canister and the resultant pressurization forces the missile out. On the other hand, to avoid damage to the bottom of the missile and the walls of the canister, cooling water or water vapor is provided to mix with the gas before they reach to close volume, which is known as the gas-steam eject launch method [1]. Thus, in order to finalize the total system design, it is necessary to understand the complicated flow structure, complex jet impingement process in a confined environment present in the launch tube. This analysis is performed with the help of powerful computers, robust numerical algorithms, computational fluid dynamics (CFD) which are made for an important role to understand this complex flow physics and help to come in an efficient design of canister system. Thus, it is necessary to authenticate the numerical tools to encounter out their range of applications and errors before using them in the design exercise [2].

To analyze the launch acceleration pulse of gas-steam ejection missile, an analysis procedure was developed by C. T. Edquist and G. L. Romine. The turbulent jet produced by the generator impinge on the canister walls, turns and initiate a recirculating flow in the canister breech which helps to create the pressurization effect to raise the missile and also holds the heating losses as well as dominating overall flow processes. The main purpose of this procedure is to analyze and modeling the loss mechanisms. In addition, both perfect and chemical gas equilibrium gas calculations were considered [3]. C.T. Edquist developed a gas dynamic model of the process involved in launching the small ICBM (Intercontinental Ballistic missile) from a canister. He thoroughly examined the launch phase and got the analytical process for examining the launch acceleration pulse of a gas-steam ejection missile and also accurately forecast the maximum load occurring during the launch. These two papers of C. T. Edquist were purely based on many assumptions of thermodynamics [1-3]. Yongquan Liu [4] studied gas-steam ejection in which the gas-steam flow (two phase and three phase) rushing into the canister including hot gas and particles of explosives, also he analyzed the gas dynamics of canister launched missile and proved that the acceleration or the pressure of the missile is uniform during the ejection of the missile. The erroneous beliefs of their simulations were small. Yongquan Liu, Anmin Xi and Hongfei Liu [5-6] also studied gas-steam ejection with different canister launched models and turbulence equations to observe the velocity and the pressure flow field in the canister. The distribution curves of the velocity and acceleration of the missile show that results of simulation in which the acceleration or pressure of the missile is more stable during launching phase. Yan Ming, Wang HanPing and Zhao ShiPing [7] carried the investigation on launching exhaust field of underwater missile, which is based on viscous non-stationary compressible phase flow theory. The simulation has been done in this investigation, which confirmed that the water injection can significantly reduce the launch barrel temperature and also increase the thrust of the missile launch. V. R. Sanal Kumar [10] carried out studies to examine the geometric dependence of transient flow features. The rapid pressurization in a canister during its starting of launch phase, the transient loads rapidly changing flow field and structural loading, and therefore has been the drive for many high-performance motors failures. The synoptic, unified modeling and simulation will provide a much more dependable and less expensive means to investigate technical issues in canister than traditional methods based on the speculative techniques. When the jet is injected into a closed cavity, it is necessary to identify the structural properties and the heat transfer by the flow by imposing it for several conditions. This types of problems are related to various practical applications including forced convection and the ventilation of mines, enclosures or corridors. Thus, the computations of heat transfer and fluid flow of turbulent plane jet injecting into a rectangular hot cavity are described by Lachacene F., Mataoui A. and Halouane [12]. Velocity and temperature distribution for the jet are computed by solving Reynolds-averaged Navier-Stokes (URANS) equations and energy-specific dissipation (k-ω) turbulence model. The heat transfer along the cavity walls is also periodic. This problem is similar, when the single phase flow, including only gas or two-phase flow, including the mixture of gas-steam are injected into the missile canister in the form of jet which is also a closed cavity.

In this research work, a single phase model (hot air) and a two-phase (air and water vapor) is proposed. In both cases, the entrance of this flow inclines to the canister at an angle of 45° to prevent the jet from impinging on the side walls directly. Also, we considered that the missile is placed at the top of canister. After the pressure in the canister reaches to the critical value, then the missile will start to move. For the single phase flow, a simulation has been done in a two-dimensional canister while for two-phase flow in a three-dimensional canister to obtain the transient flow field caused by the compressible flow.

2. Single-phase Flow Model

2.1 Introduction

Compressible flows are typically characterized by the total pressure and total temperature of the flow and described by the standard continuity, momentum and energy equations. The problem of ejecting a missile from a canister is similar to the fundamental mechanics problem of the motion of the piston in a cylinder. For the solution of this problem the basic equations required are the conservation of mass, momentum and energy in the required control volume along with transport equations of turbulence model.

Compressible flows are most often represented by the total pressure (p_0) and total temperature (T_0) of the flow. For an ideal gas, these quantities can be related to the static pressure and temperature by the following relations:

$$\frac{p_0}{p} = \exp\left(\frac{\int_T^{T_0} \frac{C_p}{T} dT}{R} \right) \tag{1}$$

For constant C_p, equation (1) reduces to,

$$\frac{p_0}{p} = \left(1 + \frac{\gamma + 1}{2} M^2 \right)^{\frac{\gamma}{\gamma - 1}} \tag{2}$$

$$\frac{T_0}{T} = 1 + \frac{\gamma + 1}{\gamma} M^2 \tag{3}$$

In the above equations the parameters p, C_p, T, R and M are represents the static pressure, specific heat, static temperature, universal gas constant and mach number respectively.

These relationships describe the variation of the static pressure and temperature in the flow as the velocity changes under isentropic conditions.

2.2 Governing Equations

Mass conservation equation:

$$\frac{\partial \rho}{\partial t} + \frac{\partial}{\partial x_i}(\rho u_i) = 0 \tag{4}$$

Momentum conservation equation:

$$\frac{\partial}{\partial t}(\rho u_i) + \frac{\partial}{\partial x_j}(\rho u_i u_j) = -\left(\frac{\partial p}{\partial x_i}\right) + \rho g + F \tag{5}$$

Energy conservation equation:

$$\frac{\partial}{\partial t}(\rho E) + \frac{\partial}{\partial x_i}(\rho u_i E + u_i p) = 0 \tag{6}$$

In the above equations (4), (5), (6), ρ, u, p, E represents the density of the gas flow, the vector of velocity, the pressure and the total energy respectively. ρg and F represents gravitational body force and external body force respectively.

To analyze the flow field inside the canister, the computer simulation has been carried out with the help of a two-equation standard k-ε turbulence model. This code solves standard k-ε turbulence equations by using simple first order implicit unsteady formulation. The standard k-ε transport equations to calculate turbulent kinetic energy (k) and turbulent dissipation rate (ε) are as follows:

$$\frac{\partial(\rho k)}{\partial t} + \frac{\partial}{\partial x_i}(\rho k u_i) = \frac{\partial}{\partial x_j}\left[\left(\mu + \frac{\mu_t}{\sigma_k}\right)\frac{\partial k}{\partial x_j}\right] + G_k - \rho\varepsilon \tag{7}$$

$$\frac{\partial(\rho \varepsilon)}{\partial t} + \frac{\partial}{\partial x_i}(\rho \varepsilon u_i) = \frac{\partial}{\partial x_j}\left[\left(\mu + \frac{\mu_t}{\sigma_\varepsilon}\right)\frac{\partial \varepsilon}{\partial x_j}\right] + C_{1\varepsilon}\frac{\varepsilon}{k}G_k - C_{2\varepsilon}\rho\frac{\varepsilon^2}{k} \tag{8}$$

In equations (7) and (8),

$C_{1\varepsilon}$= 1.44, $C_{2\varepsilon}$= 1.92, σ_k= 1.0, σ_ε= 1.3 and $G_k = \mu_t\left(\frac{\partial u_i}{\partial x_j} + \frac{\partial u_j}{\partial x_i}\right)\frac{\partial u_i}{\partial x_j}$

$C_{1\varepsilon}$ and $C_{2\varepsilon}$ are the model constants and σ_k , σ_ε are the turbulent prandtl numbers for k and ε respectively.

G_k represents generation of turbulent kinetic energy due to mean velocity gradients. The viscosity is determined from the Sutherland formula.

2.3 Computational Domain and Boundary conditions

Fig. 1 (a) represents a typical meshed model of canister in which the missile is supposed to be located on the top surface of the model. An algebraic grid generation technique is employed to discretize the computational domain. A typical grid system in the computational domain is selected after the detailed grid refinement trials. The grids are clustered near the solid walls of canister using suitable stretching functions. The clustering of the grid is maintained almost at the same level near all the solid walls of the canister. The hot air in an ideal gas state and having temperature 1,200 K is rushing into the canister through the inlet which makes an angle of 45° with the canister. As time goes by hot air starts to make the rapid pressurization in the chamber present below the missile. The missile will not be active until the force per unit area in the

Table 2. Boundary conditions

Index	Boundary conditions	Data
Inlet- Hot air (at an ideal gas state)	Velocity	35 m/s
	Temperature	1200 K
Interior field of canister	Pressure	101325 Pa
Wall	No slip, adiabatic	

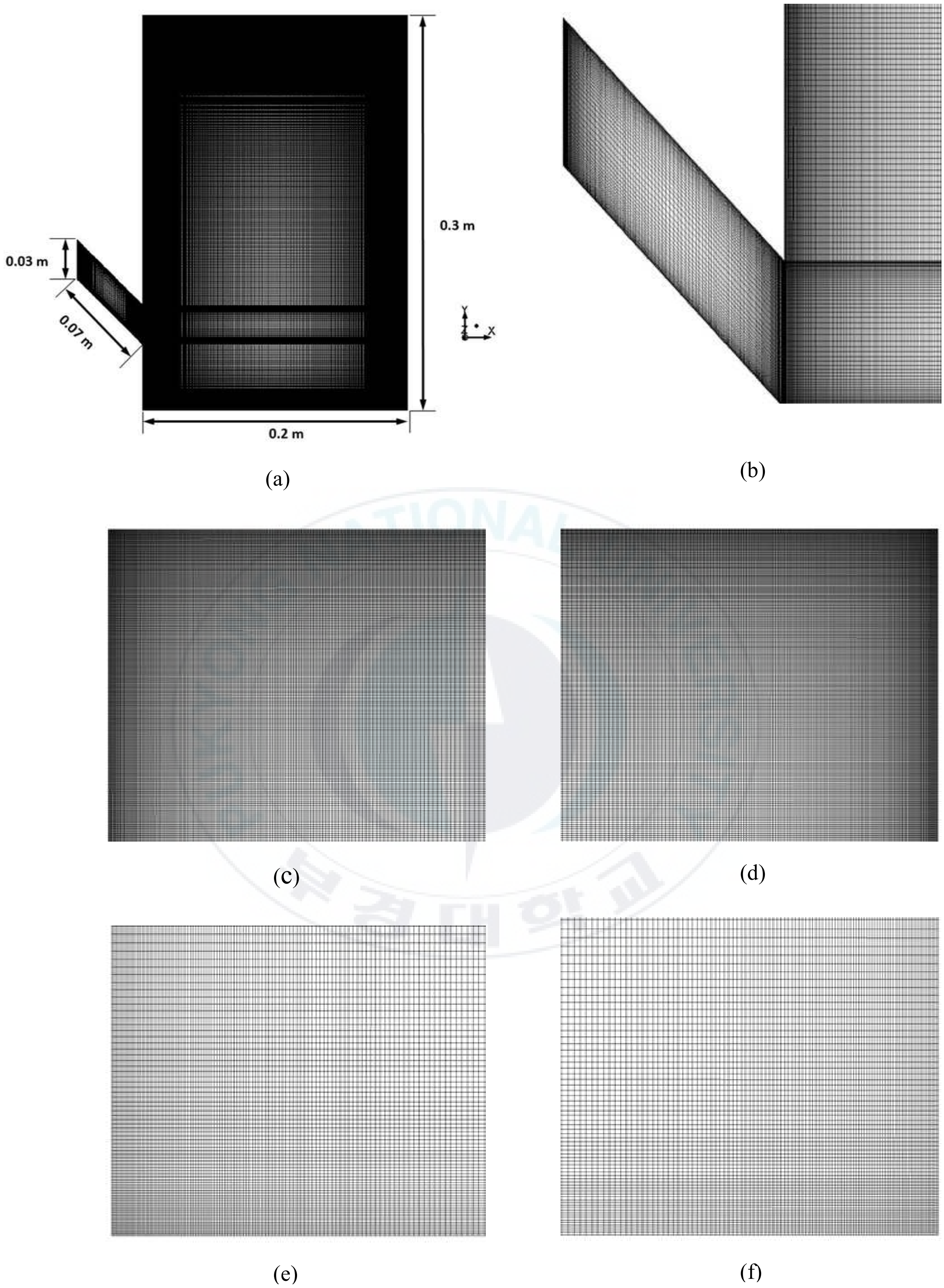

Fig. 1 (a) Typical grid in the missile-canister computational domain

(b) Inlet region (c) Top left corner (d) Top right corner

(e) Bottom left corner (f) Bottom right corne canister volume below the missile reaches to the decisive value. The time required to lift the missile depends on the flow rate or the pressure at the inlet.

The typical mesh model of the canister is well discretized into 250,142 nodes and 249,000 elements.

It was necessary to specify boundary conditions at the inlet and walls of canister. Inlet velocity was used as a boundary condition, which implies that the value of the velocity is determined as 35 m/s with inlet temperature as 1,200 K. There is no outlet for this case. The top wall of the canister is considered as a fundament of the missile. The operating pressure inside the computational domain is considered as 101,325 Pa. On walls, no slip, standard adiabatic wall functions was applied.

2.4 Results and Discussion

Contours of the total pressure in Fig. 2 representing the pressure field at 0.1 seconds. It is also showing that the pressure at the inlet is a higher magnitude than the whole pressure field in the canister. The volume of canister below the missile bottom is small and at an early stage the missile is at rest therefore as the hot gas in an ideal state is injected into the canister, with time advancement the pressure in the reservoir increases rapidly. However the no slip, adiabatic standard wall conditions were imposed on all the walls and it depicts the effect of the wall on the flow. The pressure magnitude is also influenced by the impingement of gas flow on the walls, but with the continuous gas injection the stable and enough pressure formed at the top surface of the canister which means at the bottom of the missile. The flow field conditions for the total pressure at an angle 45° are shown Fig. 2.

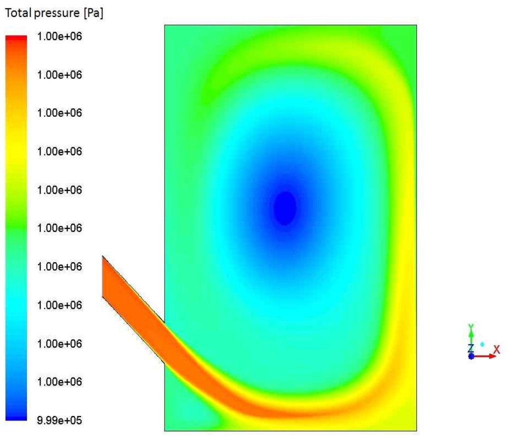

Fig. 2 Contours of total pressure at 0.1 s

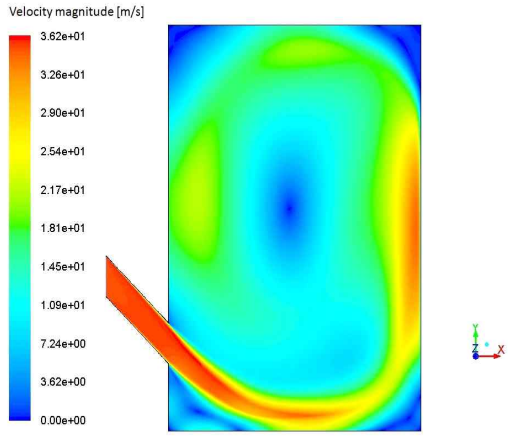

Fig. 3 Contours of velocity magnitude at 0.1 s

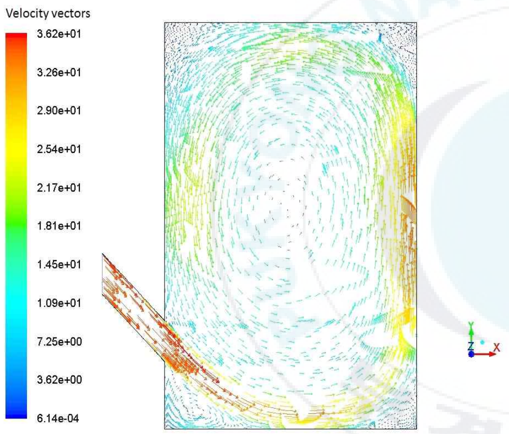

Fig. 4 Contours of velocity vectors at 0.1 s

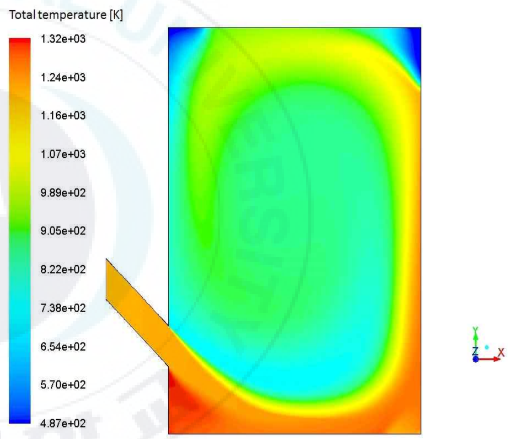

Fig. 5 Contours of total temperature at 0.1 s

The hot air in an ideal gas state rushes into the reservoir through inlet which makes an angle of 45° with the canister and it will impinge on the bottom wall. The magnitude of velocity is also influenced due to the impingements. After the consecutive impingements on the bottom, right, top and left wall the circulatory flow will form which helps to increase the rapid pressurization inside the canister. Due to some losses the velocity field becomes uniform at the bottom. The same phenomenon occurs at the other sidewalls of the canister. Before impinging at the bottom there are several eddies in the middle. Eddies in the

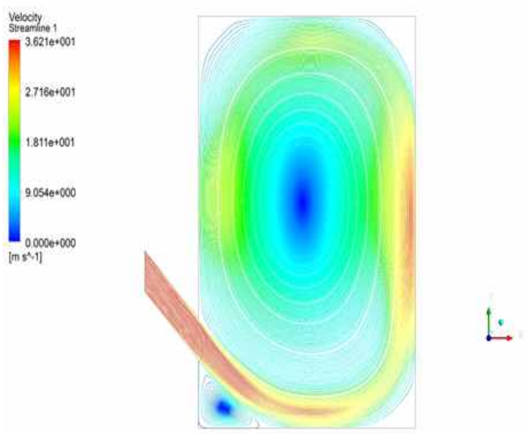

Fig. 6 Contours of streamlines at 0.1 s

gas flow will incurred at all the corners of canister which can be observed from the velocity vectors (Fig. 4). The vector plot shows that the behavior of the flow is tangential and circulatory so that the flow tends to rotate in anticlockwise direction while the direction of rotation of the eddies flow is opposite to that of the main flow at all the corners. The effects of these eddies are more dominant at bottom left corner of the canister which causes to increase the temperature in that region, i.e. it will go beyond the inlet temperature value (Fig. 5). These effects can be observed thoroughly in the flow in the form of streamlines (Fig. 6). The contours of velocity magnitude, velocity vectors, velocity streamlines clearly showing that the maximum velocity is at the inlet only while the minimum velocity is at the corners of the canister. These contours showing the velocity field under the missile at 0.1 s. The contours of velocity magnitude in the form of velocity vectors in Fig. 4 and velocity streamlines in Fig. 6 respectively, showing the direction of gas flow along the canister walls clearly.

The standard adiabatic wall conditions were applied at all the walls of the canister and hot air enters at 1,200 K. At the initial condition the temperature inside the canister is assumed as 300 K. With the sequential time steps the

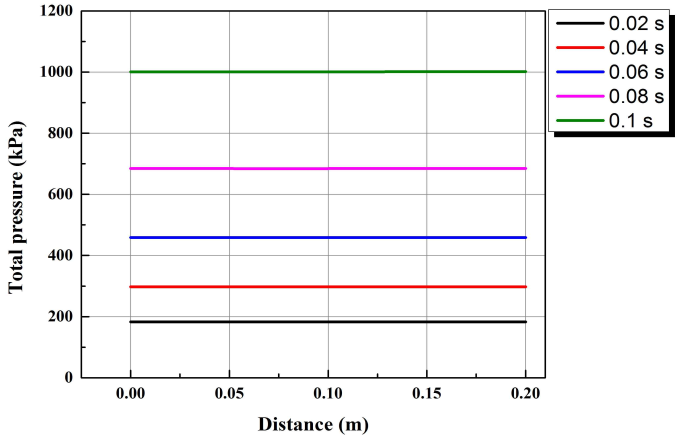

Fig. 7 Total pressure variation on top wall at different times

temperature starts to decrease due to the temperature difference between the canister inner field and hot gas temperature distribution in the canister is as shown in Fig. 5. Fig. 7 represents the total pressure distribution on top wall at different times. Initially, at 0.02 s, maximum total pressure developed at top wall is 183.15 kPa. As the time advances, i.e. at 0.04 s, 0.06 s, 0.08 s and 0.1 s the total maximum pressures developed at the top wall are 297.80 kPa, 458.68 kPa, 684.35 kPa and 1,001.11 kPa respectively. It shows that at the missile bottom, more stable and enough pressure formed at every coordinate of the top wall so that the missile will eject from the canister smoothly without any shocks. Fig. 8 explains the calculation and comparison of total temperature distribution at left and right wall. Since, the temperature is a thermodynamic property and its magnitude mainly depends upon the temperature difference between two mediums.

In this case, as the hot gas flow at 1,200 K starts to impinge on the right wall, the temperature will starts to increase in a flow region (from 0.01 m to 0.05 m). The maximum temperature of this wall at 0.1 s is found to be 1,274.49 K. After the impingement in this region the flow will move towards the top wall and from 0.05 m the temperature starts to fall and it will reach to

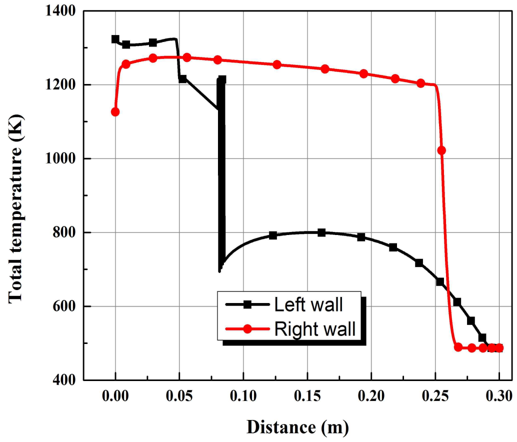

Fig. 8 Comparison of total temperature variation at left and right wall

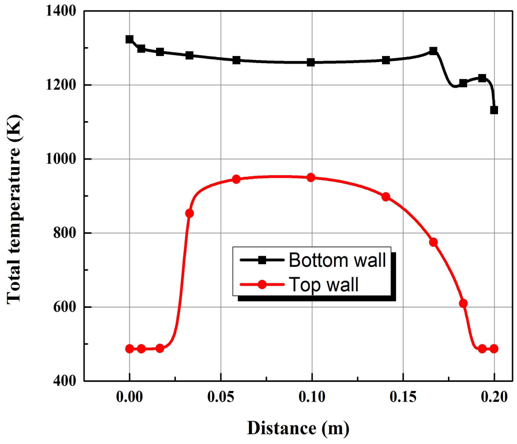

Fig. 9 Comparison of total temperature variation at top and bottom wall

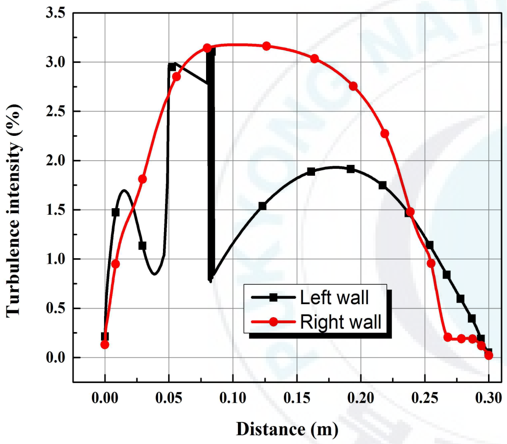

Fig. 10 Comparison of turbulence intensity at left and right wall

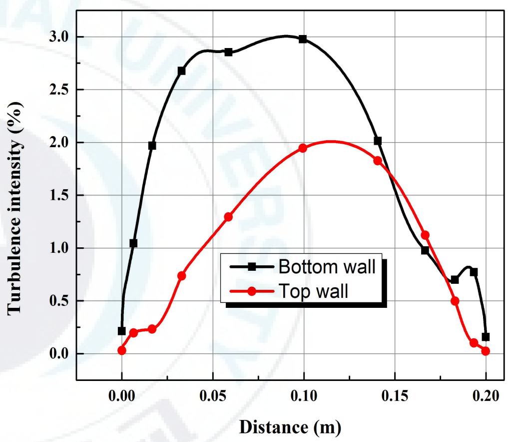

Fig. 11 Comparison of turbulence intensity at bottom and top wall

its lower value 330.57 K. As the left wall is nearby inlet, it will affected by hot gas temperature hence it shows the more temperature variation near inlet region. At bottom left corner, the temperature has higher magnitude than inlet temperature due to the effects of periodic eddy circulation in that region. The maximum and minimum temperature attained by the left wall are 1,320 K and 330.57 K respectively. According to the equations (6), (7) and (8), the variation in the temperature occurred due to the velocity changes under isentropic conditions. Fig. 9 represents the comparison of total temperature variation at the

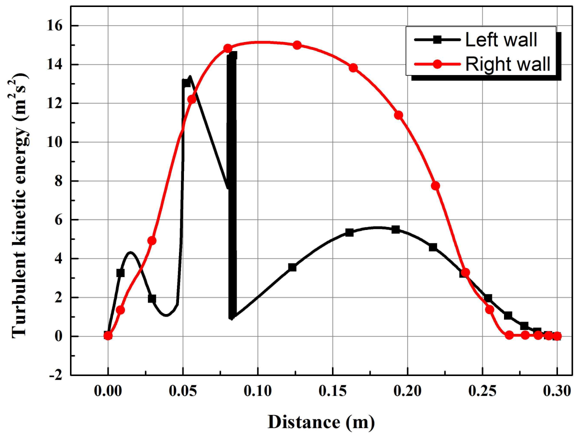

Fig. 12 Comparison of turbulent kinetic energy at left and right wall

top and bottom wall. Similar to the left wall, the bottom wall also placed near the inlet flow region. Hence, the maximum total temperature attained by this wall at 0.1 s is 1,322.83 K in the region below the inlet. While the minimum total temperature attained by this wall is 1,126.38 K at its right corner. At top wall, the maximum temperature observed is 952.57 K and the minimum temperature is 486.77 K. Fig. 10 represents the distribution and comparison of turbulence intensity at the left and right wall of the canister. Turbulence intensity is a scale characterizing turbulence expressed as a percent. An idealized flow of air with absolutely no fluctuations in air speed or direction would have turbulence intensity value of 0%. Also, it is a quantity that characterizes the intensity of gusts in the airflow. The maximum turbulence intensity of these gusts at left wall is 3.11% and it occurs at 0.08 m from the bottom while the lowest turbulence intensity is 0.03% at the end points of these walls. For right wall, the maximum and minimum turbulence intensities are 3.18% (at 0.1 m) and 0.0% (at 0.3 m) respectively. Fig. 11 represents comparison and distribution of turbulence intensity at the bottom and top walls. The maximum and minimum turbulence intensities at the bottom and top walls are 3% (at 0.09 m), 2.01% (at 0.11 m), 2% (at 0.1625 m) and 0.13%, 0.02% at its corner points

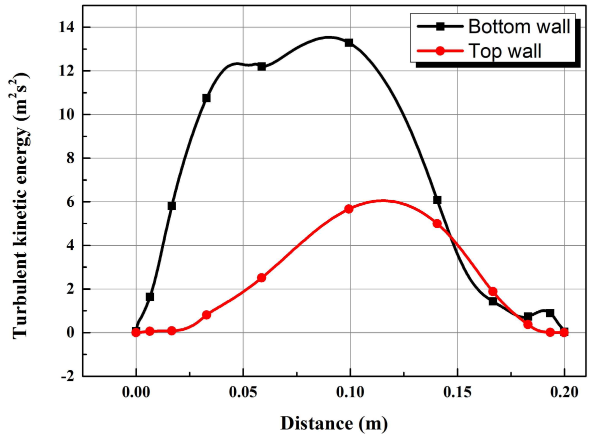

Fig. 12 Comparison of turbulent kinetic energy at bottom and top wall

respectively. From these comparisons it is cleared that the hot gas flow has more fluctuations at left and right walls as compared to the bottom and top walls. Fig. 12 represents the comparison of turbulent kinetic energy at left and right walls. Turbulent kinetic energy is generally associated with eddies in the turbulent flow and it can be produced by fluid shear, friction or buoyancy or through external forcing at low frequency eddy scales. Physically, it is characterized by measuring root-mean-square (RMS) velocity fluctuations. In this case the maximum velocity fluctuations occurred at the right wall, hence this wall bearing more turbulent kinetic energy than other walls which has a value of 15.14 m^2s^2 (At 0.11 m) as compared to all other walls while the maximum turbulent kinetic energy at left wall is 14.51 m^2s^2 (At 0.08 m). Similarly, Fig. 13 represents the comparison of turbulent kinetic energy at the bottom and top wall. The bottom wall directly struck by the hot gas flow, hence it shows the more velocity fluctuations than the top wall, hence the maximum turbulent kinetic energy at this wall is 13.54 m^2s^2 (At 0.09 m), while for the top wall its value is 6.05 m^2s^2 (At 0.11 m). The lowest turbulent kinetic energies are at the corners of the canister.

3. Two-phase Flow Model

To solve the two-phase problem, the basic equations required are the conservation of mass, momentum and energy in the control volume along with the three-dimensional transport turbulence equations as follows:

3.1 Governing Equations

<u>Mass conservation equation</u>:

$$\frac{\partial}{\partial t}(\rho_m) + \nabla.(\rho_m \vec{u}_m) = 0 \tag{9}$$

where,

$\vec{u}_m$ is the mass-averaged velocity of mixture $= \frac{1}{\rho_m}\left(\sum_{k=1}^{n}\rho_k \vec{u}_k\right)$,

ρ_m is the mixture density $= \sum_{k=1}^{n}\rho_k$,

n is the number of phases.

<u>Momentum conservation equation</u>:

$$\frac{\partial}{\partial t}(\rho_m \vec{u}_m) + \nabla.(\rho_m \vec{u}_m \vec{u}_m) = -\nabla p + \nabla.\left[\mu_m(\vec{u}_m + \vec{u}_m^T) - \frac{2}{3}\nabla.\vec{u}_m I\right] + \rho_m \vec{g} \tag{10}$$

where,

μ_m is the viscosity of mixture $= \mu_m = \sum_{k=1}^{n}\mu_k$,

$\rho_m \vec{g}$ is the gravitational body force ,

I is the unit tensor ,

$\frac{2}{3}\nabla.\vec{u}_m I$ effect of volume dilation.

Energy equation:

$$\frac{\partial}{\partial t}(\rho E) + \nabla \cdot \left[\vec{u}_m (\rho E + p) \right] = \nabla \cdot (k_{eff} \nabla T) \tag{11}$$

where,

k_{eff} is effective thermal conductivity $= [k + k_t]$,

k_t turbulent thermal conductivity ,

E_k total energy of phase k $= h_k - \frac{p}{\rho_k} + \frac{u_k^2}{2}$,

h_k sensible enthalpy for phase k (for an incompressible flow, $E_k = h_k$).

In order to analyze the gas-steam mixture flow field inside the canister, the numerical simulation has been carried out with the assistance of two equation shear-stress transport (SST) k－ω turbulence model. This model is an empirical model based on model transport equations for the turbulence kinetic energy (k) and a specific dissipation rate (ω). The SST k－ω turbulence equations are solved by using a PISO first order implicit unsteady formulation. The turbulence kinetic energy and specific dissipation rate are obtained from the following two transport equations:

$$\frac{\partial}{\partial t}(\rho k) + \frac{\partial}{\partial x}(\rho k u_i) = \frac{\partial}{\partial x}\left(\Gamma_k \frac{\partial k}{\partial x} \right) + G_k - Y_k \tag{12}$$

$$\frac{\partial}{\partial t}(\rho \omega) + \frac{\partial}{\partial x}(\rho \omega u_i) = \frac{\partial}{\partial x}\left(\Gamma_\omega \frac{\partial \omega}{\partial x} \right) + G_\omega - Y_\omega \tag{13}$$

In these equations, G_k represents the generation of turbulence kinetic energy due to mean velocity gradients. G_ω represents the generation of ω. Γ_k and Γ_ω represents the effective diffusivity of k and ω, respectively. Y_k and Y_ω

represents the dissipation of k and ω due to turbulence. The effective diffusivities for the SST k-ω model is given by,

$$\Gamma_k = \mu + \frac{\mu_t}{\sigma_k} \tag{14}$$

$$\Gamma_\omega = \mu + \frac{\mu_t}{\sigma_\omega} \tag{15}$$

where σ_k and σ_ω are the turbulent Prandtl numbers for k and ω, respectively and μ_t is the turbulent viscosity.

3.2 Computational Domain and Boundary Conditions

The three-dimensional computational domain of the missile canister is as shown in Fig. 14. The canister is a circular cylinder to which the inlet makes an angle of 45° and the missile is supposed to be placed on the top surface of the model. An algebraic grid generation technique is employed to discretize the computational domain. The grids are clustered near the solid walls of canister by using suitable stretching functions. The grids are made very fine through clustering near the wall and shear layer region to capture the important flow features accurately. A typical three-dimensional grid system has been generated first and the detailed grid refinement trials are made with proper clustering in the regions of interest. The well discretized mesh model of the canister has 193,712 nodes and 988,615 elements.

It is necessary to specify the initial conditions at the inlet and inside the computational domain and walls of the canister as mentioned in Table 2. At the inlet, mass flow rate was used as an inlet condition with the mass flow rate of 0.1 kg/s and inlet temperature as 1,200 K. There is no outlet for this case. The initial pressure and the temperature inside the computational domain are

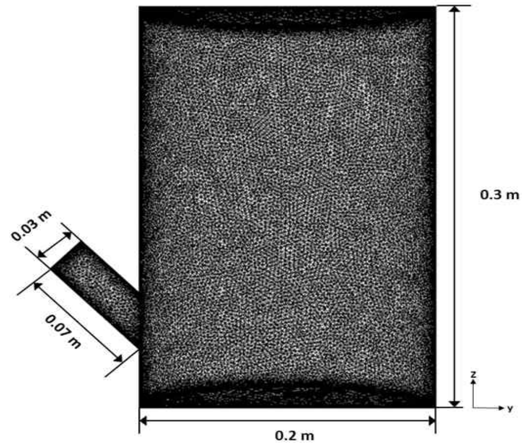

Fig. 14 3-D Meshed physical model

Table 2. Boundary conditions

Index	Boundary conditions	Data
Inlet- Hot air with water vapour	Mass flow rate	0.1 kg/s
	Temperature	1,200 K
Initial conditions	Pressure	101,325 Pa
	Temperature	300 K
Wall	No slip, adiabatic	

considered as 101,325 Pa and 300 K respectively. The top wall of the canister is considered as a bottom of the missile. On all the solid walls of canister no slip, adiabatic wall boundary conditions were applied.

3.3 Results and Discussion

The gas flow rushing into the canister is the two phase flow, including hot gas (air) and water vapor. The entrance of this mixture inclines to the canister

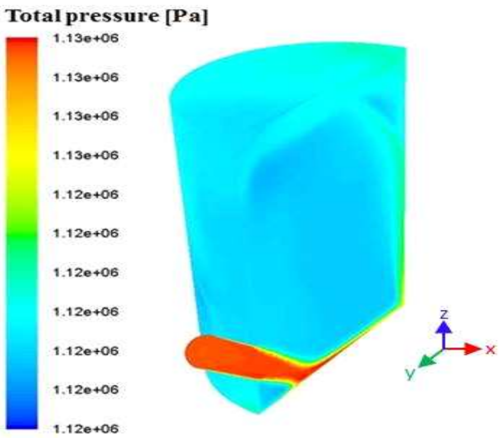

Fig. 15 Contours of total pressure at 0.1 s

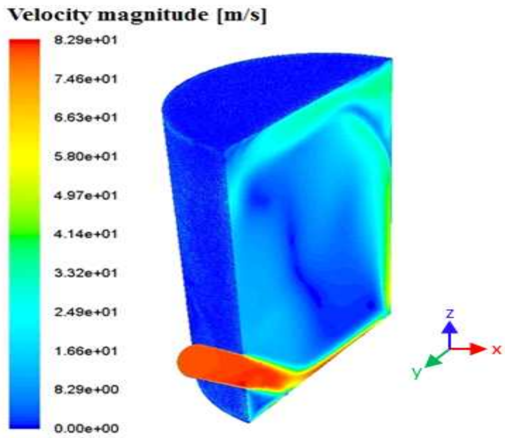

Fig. 16 Contours of velocity magnitude at 0.1 s

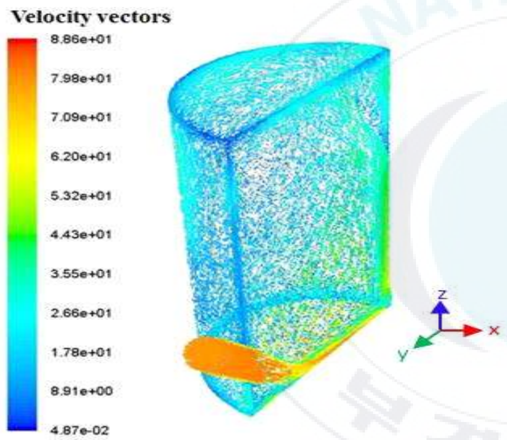

Fig. 17 Contours of velocity vectors at 0.1 s

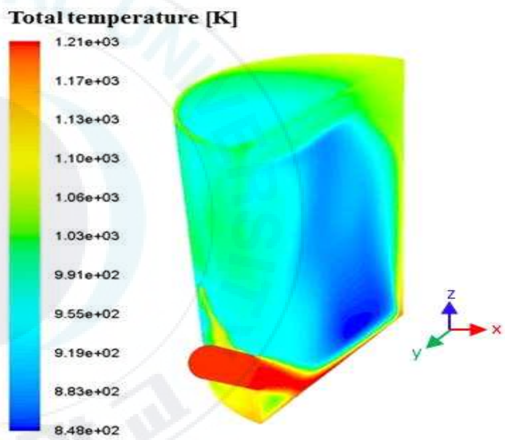

Fig. 18 Contours of total temperature at 0.1 s

at an angle of 45° to prevent the gas-steam jet from impinging on the missile and the sidewalls directly. With the time advancement, the gas-steam mixture starts to make rapid pressurization in the chamber present below the missile. The missile will not move until the pressure in a canister volume below the missile reaches the critical value. The time required to lift the missile depends on the flow rate or the pressure at the inlet. Fig. 15 illustrates the isometric view of the contours of total pressure at 0.1 s. The total maximum pressure at the inlet is 1.13×10^{6} Pa. There are some losses in pressure magnitude due to the impingement of gas-steam mixture flow on the walls, but with the continuous gas injection the stable and enough pressure formed at the bottom of missile to push it out from the canister. The maximum pressure obtained at the top wall of the canister is 1.12×10^{6} Pa and circulatory flow is generated inside the canister. Fig. 19 explains the total pressure variation on the top wall at different times. It shows that at each and every time step the uniform pressure starts to build up from 298 kPa to 1,120 kPa.

The mixture flow from the inlet enters into the computational domain with turbulence in the middle and when it approaches the bottom wall there are some losses occurring in it and the velocity field becomes uniform as shown in Fig. 16. The circulatory flow is evidenced by the calculated velocity vector at 0.1 s as shown in Fig. 17. These circulatory flows are incurred at all the corners of the canister. The vector plot confirms that there are two counter rotating circulation flow at every corner of the canister. The pressure within the two main lateral circulatory flows periodically varies inducing the deflection of the jet. The same phenomenon repeats periodically but with the continuous injection of a gas-steam mixture the tangential and circulatory flows are generated inside the canister.

The adiabatic wall boundary conditions were applied at all the walls of the canister and the flow enters at 1,200 K. The Initial condition of temperature in the computational domain is 300 K. Due to this temperature difference and the mixing of water vapor with hot air, the temperature inside the domain starts to decrease as shown in Fig. 18. The diminution of temperature can be scrutinized with the help of contours shown in Fig. 20 and Fig 21. Initially, at the bottom wall the maximum temperature was recorded as 1,200 K at the center of canister as shown in Fig. 20. As time goes by, due to the cooling effect of

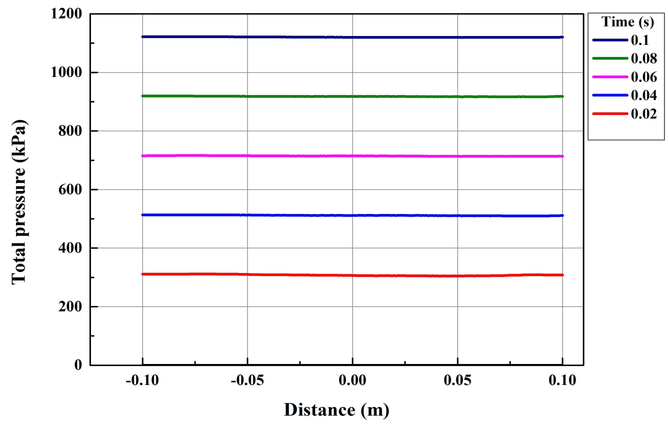

Fig. 19 Total pressure variation on top wall at different times

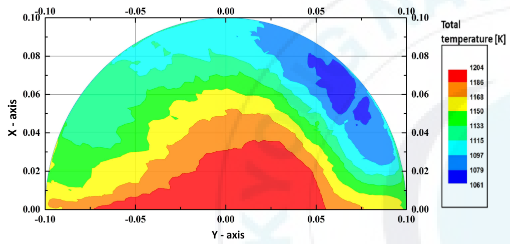

Fig. 20 Total temperature distribution at bottom wall

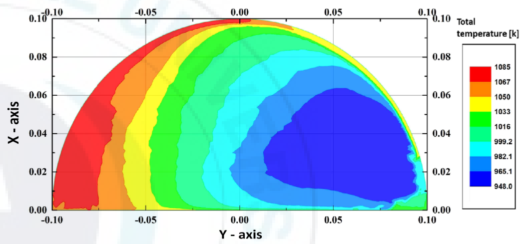

Fig. 21 Total temperature distribution at top wall

steam in canister, the hot gas temperature is reduced to the minimum temperature of 1,085 K from 1,200 K as shown in Fig. 21 which will help to avoid the damage to the missile bottom as well as launcher structure.

4. Conclusion

1. Single-phase flow model - The numerical analysis in this paper has been done with CFD code which analyzing gas flow field inside the canister. The use of two equation standard k-ε turbulence model with no slip, adiabatic wall conditions imposed on all the walls but due to the consecutive impingements, total pressure, velocity magnitude and total temperature get influenced and there were some losses due to it. Finally, This CFD code allows a reliable simulation with the uniform pressure at the bottom of missile until the missile is pushed out of the canister. This numerical simulation described the variation of total pressure, total temperature, turbulence intensities, and turbulent kinetic energies at all the walls of canister to analyze the effect these parameters during pressurization and launching conditions. This analysis will easily allow researchers studying how the changes in gas flow field will influence the canister launched missiles and found to be useful to analyze launching technologies.

2. Two-phase flow model – For this case, a comprehensive numerical simulation of the transient flow of gas-steam mixture flow in a missile canister has been conducted by solving three-dimensional SST k-ω turbulence model. In this research, we have focused on the total pressure obtained inside the canister as well as velocity and total temperature distribution inside the canister. This numerical prediction show that the uniform pressure of 1.12×10^6 Pa maintained at the missile bottom until missile will be pushed out of canister without any shocks. Sometimes the hot gas temperature leads to damage of the launcher structure for the high temperature eroding. As a result, the cooling effect, especially on the missile bottom needs further study and this simulation also addresses that the temperature at the missile bottom reduces to 1,085 K as compared to hot gas temperature (1200 K) so that hot gas will not damage the missile bottom. Notwithstanding its limitation, this simulation does confirm that the steam injection is an effective coolant with hot gas in missile canister. This model can be used to analyze the similar launch procedures.

5. References

1. Edquist, C. T., Romine, G. L., “Canister Gas Dynamics of Gas Generator Launched Missiles,” AIAA/SAE/ASME 16th Joint Propulsion Conference, AIAA-80-1186, June 30-July 2, 1980.
2. Sinha, PK., Chakraborty, D., “Numerical Study of Hot Launch of Missile Inside a Tube,” Journal of Aerospace Engineering 0 (0) 1-8.
3. Edquist, C. T., “ Prediction of the Launch Pulse for Gas Generator Launched Missiles,” AIAA/ASME/SAE/ASEE 24th Joint Propulsion Conference, AIAA-88-3290, July 11-13, 1988.
4. Liu, Y., Xi, A., “An Interior Trajectory Simulation of the Gas-steam Missile Ejection,” Journal of computers, Vol. 8, No.5, pp. 1321-1326, May 2013.
5. Liu, Y., Xi, A., Liu, H., “Numerical Study of Interior Trajectory of Missile Ejection Based on Mechanics,” Advanced Materials Research, Vol. 485 (2012), pp. 616-619, Trans Tech Publications, Switzerland.
6. Liu, Y., Xi, A., Liu, H., “An Interior Ballistic Simulation of the Gas-steam Missile Ejection,” 2010 WASE International Conference on Information Engineering.
7. Yang, M., Wang, HP., and Zhao, SP., “Simulation on Launching Exhaust Field of Underwater Missile During Vertical Hot Launching,” 2nd International Conference on Electronic & Mechanical Engineering and Information Technology (EMEIT-2012).
8. Olmsted, G. S., and Rosno, G. W., “Variable Energy Missile Eject System,” United States Patent, March 13, 1984.
9. McKinnis, J. A., O’Connell, A. R., “MX Launcher Gas Generator Concepts,” AIAA/SAE/ASME 17th Joint Propulsion Conference, AIAA-81-1577, July 27-29, 1981.

10. Sanal Kumar, V. R., Kim, H. D., Raghunandan, B. N., Setoguchi T., Raghunathan, S., " Internal Flow Simulation of High-Performance Solid Rockets using a k-ω Turbulence Model," Journal of Thermal Science, Vol. 14, No. 2.
11. Qi, Q., Chen, Q., Zhou, Y., Wang, H., Zhou, H., "Submarine-Launched Cruise Missile Ejecting Launch Simulation and Research," International Conference on Electronic and Mechanical Engineering and Information Technology, 2011.
12. Lachachene F., Mataoui A., Halouane Y., " Numerical Investigations on Heat Transfer of Self-Sustained Oscillation of a Turbulent Jet Flow Inside a Cavity," Journal of Heat Transfer, Vol. 137, October 2015.
13. Edquist C. T., " Prediction of the Launch Pulse for Gas-Generator-Launched Missiles," Martin Marietta Astronautics Group, Denver, Colorado 80201, Vol. 6, Nov.-Dec. 1990.
14. CAO Jia-yi., LU Chuan-jing., CHEN Y., CHEN Xin., LI Jie., " Research on the Base Cavity of a Sub-Launched Projectile," Journal of Hydrodynamics, 2012, 24 (2) : 244-249.
15. Hwang W. S., Choi J. Y., " Numerical Study on the Atomization process of a Supersonic Gas-Liquid Atomizer," Journal of the Korean Society for Aeronautical and Space Sciences, January 2016.
16. Lijo V., Kim H. D., Setoguchi T., Matsuo S., " Numerical Simulation of Transient Flows in a Rocket Propulsion Nozzle," January 2010, pp. 409-417.
17. Nada S. A., Fouda A., Elattar H. F., " Parametric Study of Flow Field and Mixing Characteristics of Outwardly Injected Jets into a Crossflow in a Cylindrical Chamber," International Journal of Thermal Sciences, 2016, pp. 185-201.

18. Polikhov S. A., Segal C., " Two Phase Flow Supercritical Mixing," AIAA 2006-756, 44th AIAA Aerospace Sciences Meeting and Exhibit 9-12 January 2006, Reno, Nevada.
19. Jin J. S., Yan Z. T., Hu J. M., " Modelling and Simulation of Dynamic Performance of Horizontal Steam-Launch System," Central South University and Press and Springer-Verlag Berlin Heidelberg 2013, pp. 3604-3611.
20. Coquel F., Herard J. M., Saleh K., Seguin N., " A Class of Two-Fluid Two-Phase Flow Models," AIAA 2012-3356, 42nd AIAA Fluid Dynamics Conference and Exhibit 25-28 June 2012, New Orleans, Louisiana.
21. Ariyapadi S., McMillan J., Zhou D., Berruti F., Briens C., Chan E., " Modelling the Mixing of a Gas-Liquid Spray Jet Injected in a Gas-Solid Fluidized Bed: The Effect if the Draft Tube," Chemical Engineering Science (Elsevier) 60 (2005), pp. 5738-5750.
22. Li. C., Li Y. Z., " Investigation of Entrainment Behavior and Characteristics of Gas-Liquid Ejectors Based on CFD Simulation," chemical engineering Science (Elsevier) 66 (2011), pp. 405-416.
23. Jiang Y., Li J., Yu S., Zhou F., " Cooling Effect of Water Injection on a High Temperature Supersonic Jet," Energies 2015, 8, ISSN 1996-1073.
24. Romine G., Edquist C. T., " Muzzle Blast from Canister Launched Missiles," AIAA-80-1187, AIAA/SAE/ASME 16th Joint Propulsion Conference June 30-July 2, 1980/ Hartford, Connecticut.
25. Launder B. E., Spalding D. B., " The Numerical Computation of Turbulent Flows," Computer Methods in Applied Mechanics and Engineering 3 (1974), pp. 269-289.
26. Chang S. W., Huang B. J., " Thermal Performance Improvement by Injecting Air into Water Flow," International Journal of Heat and Mass Transfer (Elsevier) 57 (2013), pp. 439-456.

27. Jayakumar J. S., Mahajani S. M., Mandal J. C., Iyer K. N., Vijayan P. K., " Thermal Hydraulic Characteristics of Air-Water Two Phase Flow in Hellical Pipes," Chemical Engineering Research and design 88 (2010), pp. 501-512.
28. Zhang X., Liu L., Cheng L., Guo Q., Zhang N., " Experimental Study on Heat transfer and Pressure Drop Characteristics of Air-Water Two Phase Flow with the effect of Polyacrylamide Additive in a Horizontal Circular Tube," International Journal of Heat and Mass Transfer 28 (2013), pp. 427-440.
29. Talley J. D., Worosz T., Kim S., " Characterization of Horizontal Air-Water Two-phase Flow in a Round Pipe Part II : Measurement of Local Two-Phase Parameters in Bubbly Flow," International Journal of Multiphase Flow 76 (2015), pp. 223-236.
30. XIAO Hu-bin, Zhao Shi-ping, " Numerical Simulation of the complex Flow Field in Combustion Gas-Steam Launching System," Journal of Solid Rocket Technology, Vol. 32, No. 4, 2009.
31. Wen W., Ying C., Lv L., Li G. H., " Numerical simulation for Gas Flow in CCL," 978-1-4244-4994-1/09 ©2009 IEEE.
32. ANSYS Fluent Theory and user Guide.

Acknowledgement

It is indeed a great pleasure and a sense of fulfillment for me to present a thesis report on,

"A Numerical Simulation on the Transient Flow of Gas-steam Mixture in a Canister"

I regard myself to be most fortunate to get an opportunity to work under the versatile and kind guidance of Prof. Jeong Soo Kim. I acknowledge a deep sense of guidance for their constant inspiration and helpful criticism.

I also thankful to our senior and elder brother Mr. Hun Jung, all laboratory members for their kindness and providing the necessary inputs at the right time.

Last but not least, no words enough to express heartiest gratitude to my beloved parents Mr. Ashok Bhosale and Mrs. Sandhya Bhosale for their support in my decision to go on to graduate studies and assistance in building up my career.

Thanking in anticipation to all readers.

Sincerely,

Bhushan Ashok Bhosale